ACCOUNTS of chemical research

Article

pubs.acs.org/accounts

Covalently-Controlled Properties by Design in Group IV Graphane Analogues

Published as part of the Accounts of Chemical Research special issue "2D Nanomaterials beyond Graphene".

Shishi Jiang,‡ Maxx Q. Arguilla,‡ Nicholas D. Cultrara,‡ and Joshua E. Goldberger*

Department of Chemistry and Biochemistry, The Ohio State University, Columbus, Ohio 43210, United States

CONSPECTUS: The isolation of graphene has sparked a renaissance in the study of two-dimensional materials. This led to the discovery of new and unique phenomena such as extremely high carrier mobility, thermal conductivity, and mechanical strength not observed in the parent 3D structure. While the emergence of these phenomena has spurred widespread interest in graphene, the paradox between the high-mobility Fermi−Dirac electronic structure and the need for a sizable band gap has challenged its application in traditional semiconductor devices. While graphene is a fascinating and promising material, the limitation of its electronic structure has inspired researchers to explore other 2D materials beyond graphene.

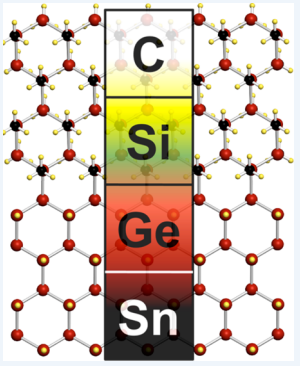

In this Account, we summarize our recent work on a new family of two-dimensional materials based on sp^3-hybridized group IV elements. Ligand-terminated Si, Ge, and Sn graphane analogues are an emerging and unique class of two-dimensional materials that offer the potential to tailor the structure, stability, and properties. Compared with bulk Si and Ge, a direct and larger band gap is apparent in group IV graphane analogues depending on the surface ligand. These materials can be synthesized in gram-scale quantities and in thin films via the topotactic deintercalation of layered Zintl phase precursors. Few layers and single layers can be isolated via manual exfoliation and deintercalation of epitaxially grown Zintl phases on Si/Ge substrates. The presence of a fourth bond on the surface of the layers allows various surface ligand termination with different organic functional groups achieved via conventional soft chemical routes. In these single-atom thick materials, the electronic structure can be systematically controlled by varying the identities of the main group elements and by attaching different surface terminating ligands. In contrast to transition metal dichalcogenides, the weaker interlayer interaction allows the direct band gap single layer properties such as photoluminescence to be readily observable without the need to exfoliate down to single layers. Furthermore, these materials can be resilient to oxidation and thermal degradation, making them attractive candidates for next generation functional materials for electronic devices and beyond.

This class of two-dimensional materials not only are promising building blocks for a variety of conventional semiconductor applications but also provide a pioneering platform to systematically and rationally control material properties using covalent chemistry. The stability and tunability of these versatile materials will push this system toward the forefront of two-dimensional research.

■ INTRODUCTION

As a result of the widespread integration of semiconductor technology into all facets of life, the group IV semiconductors, silicon and germanium, are the most important and ubiquitous materials of the current era. Not only are they the workhorse materials of transistor technology, silicon and germanium are the most prevalent materials employed in photovoltaics[1] and photodetectors[2] and have attracted considerable attention as thermoelectric energy generators.[3,4] Still, the neverending push toward device miniaturization calls for the need to understand the nature of these materials when reduced below the nanoscale. The creation of single-atom thick layers provides an avenue for the discovery of new phenomena and properties that can potentially overcome some inherent limitations in the parent three-dimensional (3D) semiconductors. For example, the indirect nature of silicon and germanium's band gap limits their efficiency in optoelectronics, and prevents their implementation into light emitting applications.

Graphene's discovery[5] has shown that it is possible to prepare single atom thick layers of a two-dimensional (2D) material, and as a consequence, numerous methods[6] have been developed to facilitate the understanding of the unique properties that emerge in single layers. Graphene is a single layer of graphite and is a comprised of a π-bonded honeycomb lattice of carbon atoms. Graphene, with its linear dispersion at the K point and massless Dirac fermions, has unique properties like high carrier mobilites (~200 000 $cm^2\ V^{-1}\ s^{-1}$), leading to the observation of the quantum hall effect at room temperature, as well as high thermal conductivity and exceptional mechanical strength.[7−9] Nevertheless, the fact that this high mobility state only appears as a result of the linear Fermi−Dirac dispersion of carbon's half-filled $2p_z$ orbitals and semimetallic zero band gap

Special Issue: 2D Nanomaterials beyond Graphene

Received: August 11, 2014
Published: December 9, 2014

DOI: 10.1021/ar500296e
Acc. Chem. Res. 2015, 48, 144−151

limits the ability to readily integrate graphene into current semiconductor technology, which requires materials with band gaps for optimal performance. For example, the lack of a band gap prevents graphene transistors from having large ratios in current between the on and off state. Functionalization of graphene to make hydrogen-terminated graphene, or graphane, opens a sizable band gap but dramatically decreases the carrier mobility to 10 $cm^2\ V^{-1}\ s^{-1}$, by bonding to the C $2p_z$ orbitals thereby eliminating the Fermi–Dirac state.[10] While graphene is a fascinating and promising material, the limitations of its electronic structure has inspired researchers to explore other 2D materials beyond graphene.

An entire field of research has emerged investigating other similar 2D van der Waals solids.[6] These materials allow for manual exfoliation to single and few-layers, breaking the weak interlayer interactions while maintaining the strong in-plane bonding. While there is an ever expanding class of these materials, this Account will primarily focus on the group IV (silicon, germanium, and tin) analogues of graphane. These structures are comprised of 2D puckered honeycomb networks of sp^3-hybridized group IV atoms and are terminated with hydrogen or other ligands (Figure 1).

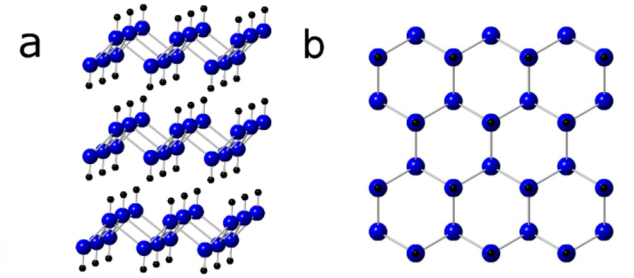

Figure 1. Model of GeH. View from (a) the (100) and (b) the (001) directions. (Ge, blue; H, black).

Although they all belong to group IV, heavier elements like Si, Ge, and Sn do not readily form π-bonds. This arises from their larger atomic size, which increases their bond distances, thereby reducing overlap between nearest neighbor π-bonding p orbitals. In other words, each Si, Ge, or Sn atom would preferentially bond to another ligand rather than form a π-bond with its neighbor. Since every atom in the 2D network has a covalently bound ligand, the identity of this ligand can provide a versatile synthetic handle for tuning the electronic structure and properties in these materials. For example, with the appropriate surface terminating ligand, these 2D materials can feature direct band gaps,[11−15] potentially enhancing silicon's and germanium's performance in photovoltaics, photodetectors, light-emitting diodes, and lasers. Furthermore, these puckered honeycomb networks are structurally analogous to Si and Ge(111) surfaces, allowing the use of established surface functionalization chemistries[16−20] to modify the ligand.

In this Account, we highlight the various routes toward synthesizing these group IV graphane analogues. We show that this system can be covalently modified with various organic functional groups. We also discuss the influence of the surface-terminating ligand and the main group element on the electronic structure and stability of these 2D materials.

TOPOTACTIC SYNTHESIS

Though the synthesis of polysilanes, polygermanes, and polystannanes from small molecules has been well developed,[21−23] they are limited to 1D inorganic polymers and single rings. To date, there have been no synthetic routes for preparing group IV graphane analogues from small molecule precursors due to the lack of a mechanism for controlling growth in two dimensions. However, the layered Zintl phases, $CaSi_2$, $CaGe_2$, and $BaSn_2$, are comprised of puckered honeycomb $[Si^-]_n$, $[Ge^-]_n$, and $[Sn^-]_n$ graphane-like layers held together by the group II $[M^{2+}]$ cations (Figure 2a).

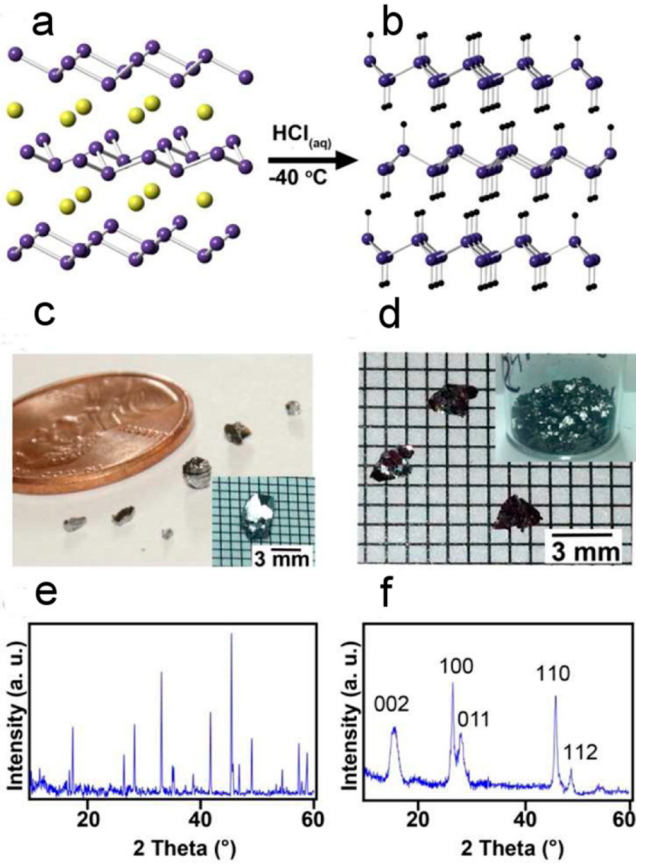

Figure 2. Schematic illustration of topotactic deintercalation of (a) $CaGe_2$ to (b) GeH (Ca, yellow; Ge, purple; H, black). Optical images of (c) $CaGe_2$ and (d) GeH crystals with select crystals on a 1 mm grid graph paper. Powder XRD of (e) $CaGe_2$ and (f) GeH.[13]

Consequently, the preparation of group IV graphane analogues relies on developing soft chemical processes that can topotactically deintercalate the M^{2+} cations while maintaining the structure and covalently terminating the anionic group IV layers.

The topotactic deintercalation of $CaSi_2$ using HCl can be traced back to Wöhler in the 1860s and Kautsky in the 1920s, and the structure and properties were partially resolved in the 1980s and 1990s.[11,12,24−29] It was reported that siloxene ($Si_6H_3(OH)_3$) preferentially forms at temperatures greater than 0 °C and layered polysilane ($Si_6H_{6-x}(OH)_{1-x}$ ($x < 1$)) forms at −30 °C.[11,12,27] These structures are silicon graphane analogues, or silicanes, with −H and −OH or mostly −H terminal substituents, respectively. Compared with the indirect band gap of crystalline silicon (1.1 eV), Siloxene has a direct band gap at

DOI: 10.1021/ar500296e
Acc. Chem. Res. 2015, 48, 144−151

around 2.4 eV with strong photoluminescence (PL).[12] Other silicon graphane analogues terminated with organic functional groups were also reported in the past decade that feature PL ranging from 2.7 to 2.9 eV.[30−32] However, all these reactions rely on the topotactic deintercalation of $CaSi_2$ in aqueous HCl, which readily produces partially OH-terminated $SiH_x(OH)_{1-x}$ due to the significantly stronger Si−O bond (800 kJ/mol) compared with the Si−H bond (300 kJ/mol). This ambiguity in surface functionalization convolutes efforts to correlate the effects of surface functionalization on the optoelectronic properties of these single-atom thick semiconductors. In contrast, the difference of bond strength is much smaller between Ge−O (660 kJ/mol) and Ge−H (320 kJ/mol) and furthermore, any native germanium oxide or hydroxide termination is readily dissolved in aqueous HCl, thereby producing pure germanane (GeH). Indeed it was reported by Brandt and Stutzmann that $CaGe_2$ thin films grown on germanium wafers can be topotactically deintercalated to form GeH, with little surface oxidation.[33]

Recently our group has synthesized for the first time millimeter-scale crystals of GeH via the topotactic deintercalation of large $CaGe_2$ single crystals in aqueous HCl (Figure 2).[13] Here, Ca^{2+} is removed via the formation of a soluble $CaCl_2$ species and the anionic $[Ge^-]_n$ layer is terminated by H atoms. X-ray diffraction (XRD) confirms that the layered hexagonal germanium lattice is maintained, and an increase in the interlayer distance occurs (5.1 to 5.5 Å) upon replacing the Ca^{2+} with two Ge−H bonds (Figure 2e,f). The large full-width at half-maximum of all the peaks that contain any *c*-axis reflections indicates that there exists a significant amount of disorder in the *c*-axis, which is common in layered materials. Pair distribution function (PDF) analysis collected from synchrotron measurements directly confirms the honeycomb 2D network of germanium atoms.[34] Compared with the PDF of crystalline Ge, GeH has systematic absences at 5.66, 7.35, and 8.95 Å (Figure 3b) that arise in 3D crystalline Ge. In Ge, these peaks correspond to Ge−Ge pairs between atoms in different (111) layers. All other peaks can be indexed to the Ge−Ge pairs within a single Ge(111) plane. The interlayer disorder of GeH prevents the observation of scattering between any interlayer Ge−Ge pairs. Furthermore, transmission electron microscopy (TEM) analysis indicates the layered morphology of GeH (Figure 3c,d). Finally, the most conclusive technique for determining the nature of the ligand bonded to each germanium atom is Fourier transform infrared spectroscopy (FTIR). Every vibrational mode observed in the FTIR corresponds to a Ge−H bond, with no peaks corresponding to any Ge−O vibrational mode. The identity of each mode was readily verified with deuterium labeling.[13]

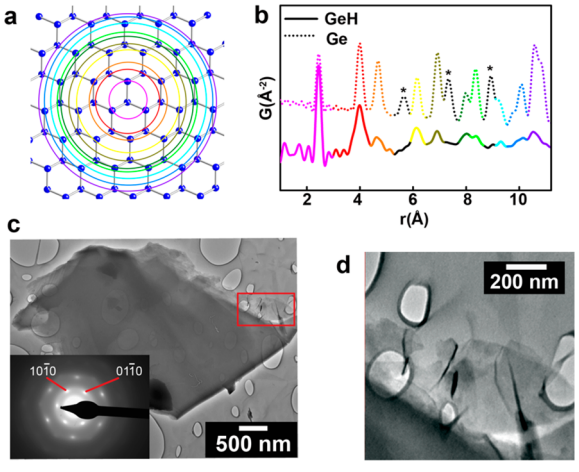

Figure 3. (a) A single (111) plane of crystalline germanium, representing a single layer of GeH. The distance of the germanium atoms on a certain colored ring from the central germanium atom corresponds to the same color peak in panel b. (b) PDFs of GeH and Ge. The starred peaks correspond to the interactions between germanium atoms in different layers.[34] (c) Low-magnification and (d) magnified TEM micrograph of GeH platelets. Inset in panel c is the corresponding electron diffraction pattern collected down the [001] zone axis.[13]

The deintercalation of Zintl phases that contain multiple group IV elements enables the synthesis of alloy graphane analogues. We have been able to substitute up to 9% of the Ge atoms with Sn (Figure 4a) in the precursor Zintl phase

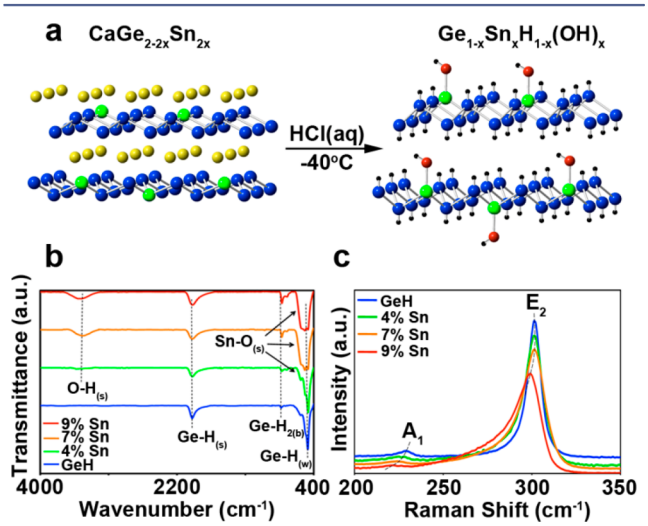

Figure 4. (a) Topotactic deintercalation of $CaGe_{2-2x}Sn_{2x}$ to $Ge_{1-x}Sn_xH_{1-x}(OH)_x$ in HCl (Ca, yellow; Ge, blue; H, black; O, red; Sn, green). (b) FTIR and (c) Raman spectra of $Ge_{1-x}Sn_xH_{1-x}(OH)_x$ (x = 0−0.09).[35]

($CaGe_{2-2x}Sn_{2x}$).[35] Deintercalation in aqueous HCl produces a 2D honeycomb network where tin is OH-terminated while germanium remains H-terminated (Figure 4b). Raman spectroscopy confirms that alloying occurs, because the shifts in both the in-plane phonon (E_2) and cross-plane (A_1) vibrational modes are consistent with the expected differences based on the changes in the reduced mass (Figure 4c).

Single and Few Layer Thick Materials

The synthesis of large millimiter-scale flakes of GeH enables the isolation of single and few layer thick sheets via mechanical exfoliation using polydimethylsiloxane (PDMS) and Scotch tape (Figure 5a), by adapting the procedure developed by Frindt.[36,37] These single-layer flakes were exfoliated onto 110 nm thick and 300 nm thick SiO_2/Si substrates, which provide suitable optical contrast. However, mechanical exfoliation is a labor-intensive and nonscalable process for producing single and few-layer thick materials. Additionally, the interlayer van der Waals interactions in GeH are calculated to be ∼35% stronger in GeH compared with graphene,[13] which experimentally makes the preparation of large areas of single layer GeH more challenging. The ability to synthesize precise layer thicknesses of these group IV graphane analogues on Si and Ge

DOI: 10.1021/ar500296e
Acc. Chem. Res. 2015, 48, 144−151

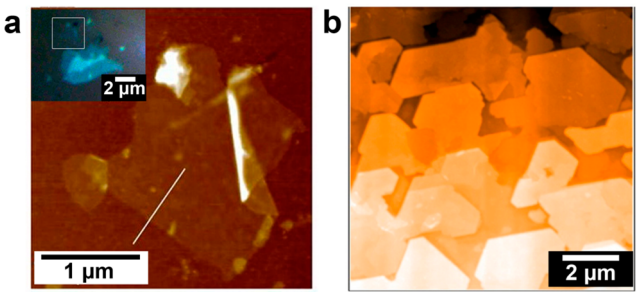

Figure 5. AFM images of (a) an exfoliated single layer of GeH and (b) GeH thin film after deintercalation of a 5 nm thick $CaGe_2$ film grown via MBE on Ge(111). Inset in panel a is an optical micrograph of the single-layer flake.[13,38]

substrates, would enable their seamless integration into existing semiconductor fabrication infrastructure. This can be achieved by first epitaxially growing the precursor Zintl phases onto Si and Ge substrates. The *a*,*b*-parameters of the precursor $CaGe_2$ Zintl phase closely match the spacing of the Ge(111) surface to less than 0.5%. This enables the direct epitaxial growth of $CaGe_2$ thin films on Ge(111) wafers, which can be subsequently topotactically deintercalated to obtain GeH. Indeed, we have prepared 5 nm thick films of $CaGe_2$ on Ge(111) via molecular beam epitaxy (MBE), which would correspond to ~10 layers.[38] These co-deposited $CaGe_2$ thin films have grain sizes on the order of a few micrometers, which is the typical size of terrace formed due to the miscut of the Ge(111) growth substrate. Upon treatment in HCl, these thin films exhibit the same XRD and Raman profiles as those produce from single crystals of $CaGe_2$. Consequently, the combination of epitaxial growth and topotactic deintercalation represents a promising and scalable route for the preparation of precise layer films of group IV graphane analogues and simplifies subsequent very large scale integration (VLSI) processing.

■ COVALENTLY MODIFIABLE BUILDING BLOCKS

The presence of a covalently bound surface ligand on every atom in these group IV graphane analogues opens up the possibility of tuning the properties by varying this surface ligand. There has been extensive work during the past few decades showing that every atom on Si and Ge(111) surfaces can be terminated with small organic substituents such as $-CH_3$ and $-CCH$.[16−20,39] In contrast to H-terminated Si/Ge(111) surfaces, which oxidize within 30 min of exposure to air, these organic-terminated surfaces have been shown to be resistant toward oxidation for at least 30 days.[19,39,40] Consequently, it is easy to envision 2D derivatives of these same organic functionalized surfaces.

To these ends, we have developed a one-step metathesis approach that directly converts $CaGe_2$ crystals into organic-terminated germananes by topotactically reacting them with organoiodines. For instance, we have prepared ~1 mm flakes of $GeCH_3$ (Figure 6a,b) by reacting $CaGe_2$ with CH_3I.[14] Through this reaction, Ge^- anions bond to the CH_3 group, and the iodide reacts with Ca^{2+} to form a soluble CaI_2 species, which is easily separated. Single crystal and powder XRD analysis show that the hexagonal unit cell of $CaGe_2$ is retained and $GeCH_3$ has a similar 2H unit cell (two $GeCH_3$ layers per unit cell) as GeH (Figure 6c,d). The interlayer distance of $GeCH_3$ is increased by 3.1 Å compared with GeH, which is close to the

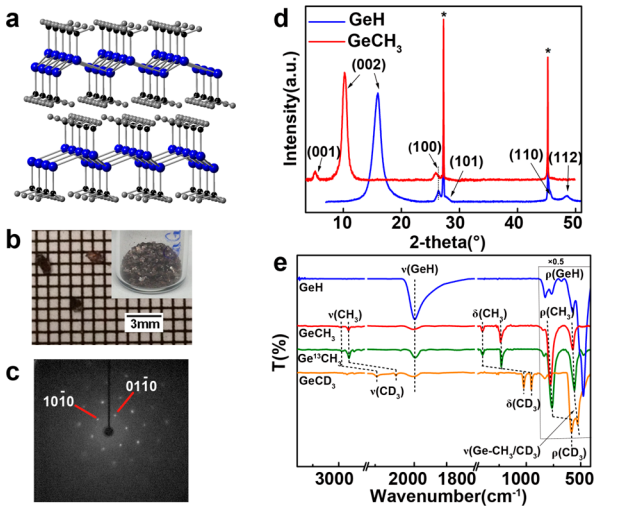

Figure 6. (a) Model of $GeCH_3$ (Ge, blue; C, black; H, gray). (b) Optical images of $GeCH_3$ crystals with select crystals on 1 mm grid graph paper. (c) Single-crystal XRD pattern of $GeCH_3$ collected down the [001] zone axis. (d) Powder XRD pattern of GeH and $GeCH_3$. The starred peaks correspond to diffraction reflections of an internal Ge standard. (e) FTIR spectra of GeH, $GeCH_3$, $Ge^{13}CH_3$, and $GeCD_3$. The intensities of the four spectra are multiplied by 0.5 from 400 to 900 cm^{-1}.[14]

estimated increase (~2.5 Å) based on the bond length and van der Waals radii differences of these two ligands. The methyl termination is further confirmed by FTIR measurements (Figure 6e). Compared with spectra of GeH, the intense Ge−H stretching mode at 2000 cm^{-1} is almost entirely gone, while a Ge−C stretching mode at 573 cm^{-1} is observed. Other vibrational modes like $-CH_3$ stretching, bending, and rocking modes are also detected. The identity of each mode can be further verified upon comparison with the FTIR spectra of $Ge^{13}CH_3$ and $GeCD_3$.

This one-step metathesis method is a general route for preparation of organic ligand terminated germananes. By substituting CH_3I with other organoiodine reagents like CH_3CH_2I and $CH_2{=}CHCH_2I$, we have prepared CH_3CH_2Ge and $CH_2{=}CHCH_2Ge$, respectively. The interlayer spacing is expected to increase by 3.5 and 6.2 Å, upon replacing −H in GeH with $-CH_2CH_3$ and $-CH_2CH{=}CH_2$, respectively. This is in close agreement with the increases in interlayer spacing of 3.7 and 5.8 Å observed via XRD (Figure 7a). In FTIR spectra, Ge−C stretching can be detected in all three spectra along with the near elimination of the Ge−H stretching mode. All the other vibrational modes can be assigned to the corresponding

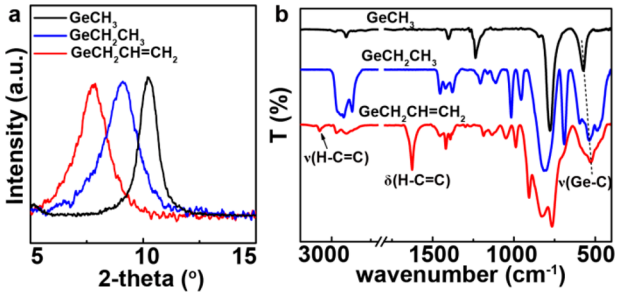

Figure 7. (a) Powder XRD pattern and (b) FTIR spectra of $GeCH_3$ (black), $GeCH_2CH_3$ (blue), and $GeCH_2CH{=}CH_2$ (red).

DOI: 10.1021/ar500296e
Acc. Chem. Res. 2015, 48, 144−151

organic functional groups. The observation of H−C═C− stretching and bending modes at 3076 and 1626 cm^{-1} further confirms the termination with $-CH_2CH{=}CH_2$. The versatility of this reaction scheme enables the grafting of functional ligands with tunable polarity, reactivity, and mechanical strength for a wide variety of applications.

TUNING THE ELECTRONIC STRUCTURE

The rich surface functionalization chemistry allows these group IV graphane analogues to be highly tunable electronic and optoelectronic building blocks for next generation devices. By substituting the main group element and varying the surface ligand, one can tune the electronic structure of these materials to produce unique properties that do not exist in the parent 3D semiconductor structure. To understand how the presence of a surface ligand influences the electronic structure of these 2D graphane analogues, here we describe density functional theory (DFT) simulations illustrating the difference between silicene and silicane as a model system.[41,42]

Silicene is a 2D material comprised of a honeycomb arrangement of Si atoms in which every Si shares three σ and one π bond with the three neighboring Si atoms.[42,43] Similar to graphene, this structure exhibits Fermi−Dirac behavior at the K point on account of the half-filled $3p_z$ orbitals (Figure 8a).

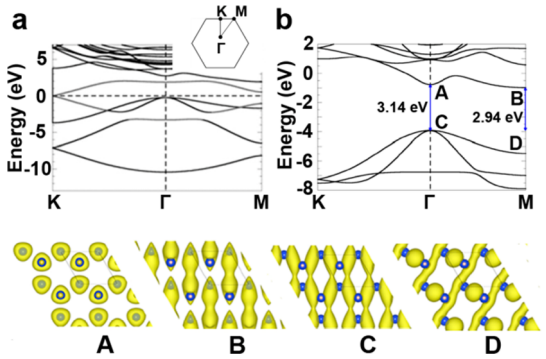

Figure 8. DFT simulations of the electronic band structure of (a) silicene and (b) silicane and the density orbitals at the high symmetry k-points: (A) Si−H σ*, (B) Si−Si σ*, (C, D) Si−Si σ states. Inset in panel a is the hexagonal Brillouin zone.[42]

Adding hydrogen as a surface terminating ligand to silicene produces silicane (SiH) through the formation of a covalent bond with the Si $3p_z$ orbital.[42−44] This bonding and antibonding interactions splits the Dirac cone at the K point thus opening a sizable band gap (Figure 8b). The electronic band structure of silicane calculated at the HSE-06[45,46] level predicts an indirect band gap of 2.94 eV from Γ to M and a direct band gap of 3.14 eV at Γ.[42] The conduction band valley at Γ is comprised of Si−H σ* states, the conduction band minimum (CBM) at M corresponds to Si−Si σ* states, whereas the valence band maximum (VBM) corresponds to Si−Si σ states (Figure 8b).

The band structures of GeH and SnH are closely related to SiH.[42,43] However, in the case of GeH, the CBM occurs at Γ and not M, leading to a 1.56 eV direct band gap with an effective electron mass of $m_{e,\Gamma}$* = 0.09. This is consistent with the observed absorption onset at 1.59 eV and with the observation of PL in GeH at 1.56 eV at low temperature. The direct band gap of GeH is in sharp contrast to the 0.67 eV indirect bap gap of crystalline germanium.[47] In crystalline germanium, the CBM occurs in the four equivalent valleys at the L ⟨111⟩ point, which has a much higher effective mass ($m_{e,L}$* = 1.64) than the conduction band valleys at Γ ($m_{e,\Gamma}$* = 0.041). However, since GeH can be thought of as hydrogen-terminated isolated (111) sheets of germanium, we are effectively eliminating the L wavevector in the Ge Brillouin zone, resulting in a material that has a direct gap and a considerably higher electron mobility. Electron mobility is inversely proportional to effective mass. We calculated from first-principles the phonon-limited electronic mobility for an isolated single layer of GeH obtaining a room temperature mobility of ∼18000 $cm^2\ V^{-1}\ s^{-1}$. This 5× increase in electron mobility from bulk Ge (3900 $cm^2\ V^{-1}\ s^{-1}$) is consistent with the reduced electron effective mass in GeH. These group IV graphane analogues also feature significantly larger band gaps compared with the parent 3D material (Table 1).

Table 1. Band Gaps of Different sp^3-Hybridized Group IV Elements in Bulk and in 2D

	3D sp^3 (eV)	2D sp^3 (eV)
C	5.48 (indirect)[48]	3.5[a] (−H, direct)[49]
Si	1.12 (indirect)[50]	2.4 (−OH/−H, direct),[11] 2.94[a] (−H, indirect)[42]
Ge	0.67 (indirect)[47]	1.59 (−H, direct)[13] 1.71 ($-CH_3$, direct)[14]
Sn	0 ± 0.05 (β-, direct)[51]	∼0.30[a] (−H, −halides, direct)[15]

[a]Theoretical.

The 2D sp^3-hybridized Sn is predicted to be a topological insulator when terminated by electronegative groups such as −OH and various halides, yet remains as a trivial insulator when terminated by smaller less electronegative ligands such as −H.[15] This topological phase emerges when the Sn 5s σ* bands drop below the $4p_x$ and $4p_y$ VBM, which is split on account of the large spin−orbit coupling in Sn. Consequently, 2D tin is predicted to exhibit the quantum spin Hall effect.

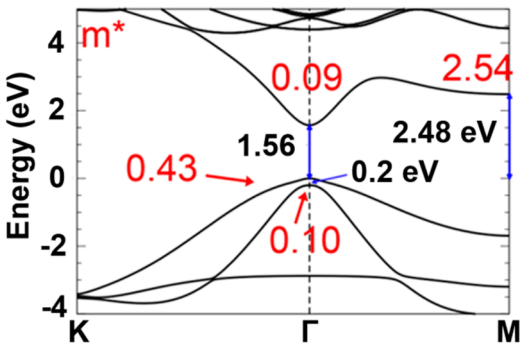

Figure 9. Electronic band structure of an isolated single layer of GeH calculated using HSE-06 theory including spin−orbit coupling predicting a 1.56 eV direct band gap. The hole and electron effective masses for each extrema are indicated in red.[13]

One way to tune the electronic structure of these 2D materials is through alloying different group IV elements in the framework. We have systematically tuned the band gap of GeH from 1.59 eV down to 1.38 eV (Figure 10a,b) through alloying up to 9% Sn into the $CaGe_{2-2x}Sn_{2x}$ lattice and topotactically deintercalating the lattice with aqueous HCl, based on of diffuse reflectance absorption (DRA) measurements.[35] Increasing the Sn percentage in the lattice can potentially lead to band gaps

DOI: 10.1021/ar500296e
Acc. Chem. Res. 2015, 48, 144−151

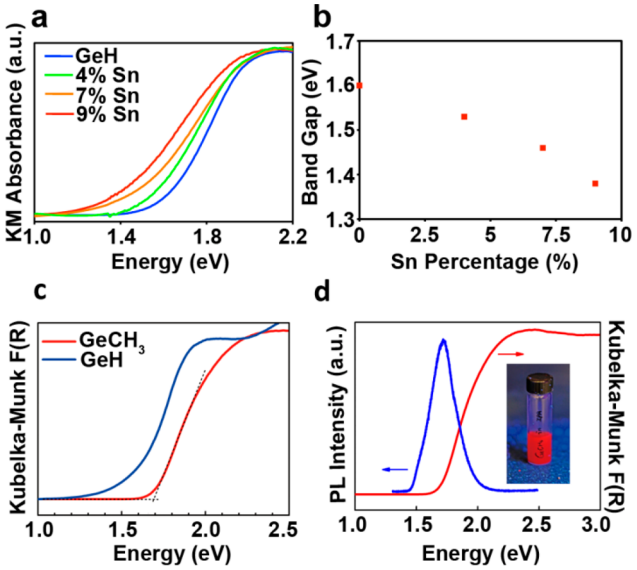

Figure 10. (a) DRA spectra of $Ge_{1-x}Sn_xH_{1-x}(OH)_x$ (x = 0 to 0.09) plotted in terms of the Kubelka–Munk function illustrating the consistent red shift in the absorption onset.[35] (b) Sn-dependent optical band gap of $Ge_{1-x}Sn_xH_{1-x}(OH)_x$ alloys obtained via a linear approximation of the absorption edge.[35] (c) DRA spectra of GeH compared with $GeCH_3$ and (d) absorption and PL spectra of $GeCH_3$ with the actual PL observed in isopropyl alcohol as an inset.[14]

down to 0.3 eV, which would open up their application as tunable photodetectors suitable for telecommunications.

Aside from alloying the main group element, another route that can be used to tune the properties of these materials is through the variation of the surface ligand. Because the CBM at Γ corresponds to the group IV–ligand σ^* antibond, this energy level can be raised or lowered depending on the electronegativity of the surface terminating ligand. Since the ligand also influences the geometry of the entire lattice, this also leads to changes in the bond lengths and bond angles in the 2D network, significantly affecting the rest of the band structure. Therefore, substituting one ligand for another will affect the entire electronic band structure and can significantly change the observed band gap and direct/indirect nature. A systematic experimental study comparing the electronic and optical properties of uniformly functionalized 2D group IV graphane analogues is needed to foster a deeper understanding of the influence of surface ligands on the electronic structure of these materials.

Experimentally, we have demonstrated that the band gap of GeH can be increased by 0.1 eV (Figure 10c) by replacing the −H with $-CH_3$.[14] Furthermore, very intense band edge PL is observed in $GeCH_3$ (Figure 10d) with a quantum yield of 0.2%. In contrast to other layered materials like MoS_2, this PL is independent of layer thickness, thus obviating the need for large area single layers for practical devices. The change in PL indicates that optical properties of these 2D group IV graphane analogues can potentially be improved with different ligand terminations. In summary, the combination of alloying and covalent functionalization provides an unprecedented level of control over electronic structure in a 2D crystal, creating a versatile platform for electronic and optoelectronic applications.

THERMAL AND AIR STABILITY

The potential utility of these group IV graphane analogues for any functional device strongly hinges on their air and temperature stability. It has been established that silicon-based 2D systems such as SiH readily oxidize upon exposure to air.[31,44] GeH, however, shows a remarkable resistance to oxidation.[13] The lack of oxidation in the bulk material is observed in FTIR measurements (Figure 11a) after air

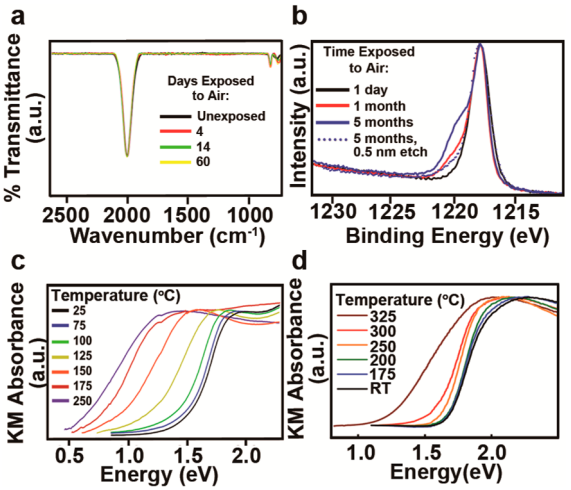

Figure 11. (a) FTIR spectra of GeH after exposure to air for up to 60 days highlighting the absence of any Ge–O vibrational mode. (b) XPS spectra of GeH exposed to air for up to five months, followed by 0.5 nm Ar etch. DRA spectra of (c) GeH and (d) $GeCH_3$ annealed in Ar/H_2 gas at various temperatures.[13,14]

exposure of up to 60 days where the absence of different GeO_x vibrational modes[S2] from 800 to 1000 cm^{-1} indicate that the bulk of GeH is unchanged. On the other hand, X-ray photoelectron spectroscopy (XPS) (Figure 11b) is the most sensitive technique in determining the presence of oxidation on the surface. After five months of exposure to air, a $Ge^{2+/3+}$ shoulder emerges at 1219.3 eV (29.7% $Ge^{2+/3+}$) indicating that surface oxidation is prevalent. After Ar ion etching of the top 0.5 nm (~1 layer), the $Ge^{2+/3+}$ peak almost completely disappears with 10.1% $Ge^{2+/3+}$ remaining.[13] Together, the XPS and FTIR mothers suggest that GeH is resilient toward oxidation and only the surface layer slowly oxidizes.

The thermal stability of these 2D materials strongly depend on the identity of the surface terminating ligand. We observed that in GeH, the emergence of thermal-induced amorphization begins at 75 °C.[13] We have observed that measurements focused on changes in properties are the most sensitive methods for detecting amorphization, compared with bulk structural analyses like XRD and Raman spectroscopy. The absorption of the new and emerging amorphous germanium species lower than the 2D germanane band gap is more readily observable than the gradual disappearance of a crystalline phase in XRD or Raman. Upon annealing at 75 °C and above, there is an increasing red shift in the absorption onset, consistent with the formation of amorphous GeH and, at higher temperatures, amorphous Ge (Figure 11c).[13] This amorphization process was further confirmed with temperature dependent PDF measurements.[34] In contrast, $GeCH_3$ starts to amorphize at a significantly higher annealing temperature, at around 250 °C (Figure 11d).[14] In summary, the oxidation resistance of germanane and the improvement in thermal stability by methyl

DOI: 10.1021/ar500296e
Acc. Chem. Res. 2015, 48, 144–151

termination makes these materials attractive candidates for next generation devices and can be potentially robust enough to withstand the demands for fabrication and operation.

CONCLUSION AND OUTLOOK

These group IV graphane analogues are real materials that can be synthesized as robust single crystals in gram-scale quantities, exfoliated into single layers, and prepared on conventional VLSI substrates as few-layer thin films. Compared with all other 2D van der Waals solids, these group IV graphane analogues offer the capability for covalent surface termination, providing a versatile handle for tailoring the structure, stability, and electronic properties in single-atom-thick materials. Such exquisite control over the material properties makes these systems attractive candidates for a multitude of applications such as sensing, optoelectronics, and thermoelectrics and also offers the potential for new physical phenomena such as the quantum spin Hall effect. Leveraging previously established semiconductor surface functionalization routes will enable the creation of entire libraries of organic ligand terminated 2D materials. Overall, this new class of 2D materials is posed to have a great impact not only in the traditional sectors of nanoscience but also in opening up a new research paradigm in covalently controlled properties by design.

AUTHOR INFORMATION

Corresponding Author

*E-mail: goldberger@chemistry.ohio-state.edu.

Author Contributions

‡S.J., M.Q.A., and N.D.C. contributed equally.

Notes

The authors declare no competing financial interest.

Biographies

Shishi Jiang received her B.S. (2011) in chemistry from University of Science and Technology of China. She is currently working towards her Ph.D. in Chemistry from The Ohio State University. Her research focuses on the covalent functionalization of group IV graphane analogues.

Maxx Arguilla received his B.S. degree from the University of the Philippines-Diliman in 2011. He is currently a graduate student in the Chemistry department of The Ohio State University. His research mainly focuses on germanium/tin alloys and tin-based group IV graphane analogues.

Nicholas Cultrara received a B.S. from State University of New York, University at Buffalo, in 2012 and is currently working towards his Ph.D. in Chemistry at The Ohio State University. His research primarily focuses on the doping and electronic characterization of group IV graphane analogues.

Joshua Goldberger received his B.S. from The Ohio State University in 2001 and his Ph.D. in Chemistry from University of California, Berkeley, in 2006. He did postdoctoral research at Northwestern University before joining the faculty in the Department of Chemistry at The Ohio State University in 2010. His main research interests focus on solid-state materials at the atomic scale, and their applications in electronics, energy conversion, and photonics. More information about the Goldberger group can be found at http://research.chemistry.ohio-state.edu/goldberger/

ACKNOWLEDGMENTS

We graciously acknowledge Wolfgang Windl for DFT simulations. The materials development was supported by the Army Research Office (Grant W911-NF-12-1-0481), and the simulations were supported by the Center for Emergent Materials at The Ohio State University, an NSF MRSEC center (Grants DMR-0820414 and DMR-1420451).

REFERENCES

(1) Lalović, B.; Kiss, Z.; Weakliem, H. A Hybrid Amorphous Silicon Photovoltaic and Thermal Solar Collector. *Sol. Cells* **1986**, *19*, 131−138.

(2) Auston, D. H.; Lavallard, P.; Sol, N.; Kaplan, D. An Amorphous Silicon Photodetector for Picosecond Pulses. *Appl. Phys. Lett.* **1980**, *36*, 66−68.

(3) Joshi, G.; Lee, H.; Lan, Y.; Wang, X.; Zhu, G.; Wang, D.; Gould, R. W.; Cuff, D. C.; Tang, M. Y.; Dresselhaus, M. S.; Chen, G.; Ren, Z. Enhanced Thermoelectric Figure-of-Merit in Nanostructured p-type Silicon Germanium Bulk Alloys. *Nano Lett.* **2008**, *8*, 4670−4674.

(4) Hochbaum, A. I.; Chen, R.; Delgado, R. D.; Liang, W.; Garnett, E. C.; Najarian, M.; Majumdar, A.; Yang, P. Enhanced Thermoelectric Performance of Rough Silicon Nanowires. *Nature* **2008**, *451*, 163−167.

(5) Novoselov, K. S.; Geim, A. K.; Morozov, S. V.; Jiang, D.; Zhang, Y.; Dubonos, S. V.; Grigorieva, I. V.; Firsov, A. A. Electric Field Effect in Atomically Thin Carbon Films. *Science* **2004**, *306*, 666−669.

(6) Butler, S. Z.; Hollen, S. M.; Cao, L.; Cui, Y.; Gupta, J. A.; Gutiérrez, H. R.; Heinz, T. F.; Hong, S. S.; Huang, J.; Ismach, A. F.; Johnston-Halperin, E.; Kuno, M.; Plashnitsa, V. V.; Robinson, R. D.; Ruoff, R. S.; Salahuddin, S.; Shan, J.; Shi, L.; Spencer, M. G.; Terrones, M.; Windl, W.; Goldberger, J. E. Progress, Challenges, and Opportunities in Two-Dimensional Materials beyond Graphene. *ACS Nano* **2013**, *7*, 2898−2926.

(7) Novoselov, K. S.; Geim, A. K.; Morozov, S. V.; Jiang, D.; Katsnelson, M. I.; Grigorieva, I. V.; Dubonos, S. V.; Firsov, A. A. Two-Dimensional Gas of Massless Dirac Fermions in Graphene. *Nature* **2005**, *438*, 197−200.

(8) Balandin, A. A.; Ghosh, S.; Bao, W.; Calizo, I.; Teweldebrhan, D.; Miao, F.; Lau, C. N. Superior Thermal Conductivity of Single-Layer Graphene. *Nano Lett.* **2008**, *8*, 902−907.

(9) Lee, C.; Wei, X.; Kysar, J. W.; Hone, J. Measurement of the Elastic Properties and Intrinsic Strength of Monolayer Graphene. *Science* **2008**, *321*, 385−388.

(10) Elias, D. C.; Nair, R. R.; Mohiuddin, T. M. G.; Morozov, S. V.; Blake, P.; Halsall, M. P.; Ferrari, A. C.; Boukhvalov, D. W.; Katsnelson, M. I.; Geim, A. K.; Novoselov, K. S. Control of Graphene's Properties by Reversible Hydrogenation: Evidence for Graphane. *Science* **2009**, *323*, 610−613.

(11) Yamanaka, S.; Matsu-ura, H.; Ishikawa, M. New Deintercalation Reaction of Calcium from Calcium Disilicide. Synthesis of Layered Polysilane. *Mater. Res. Bull.* **1996**, *31*, 307−316.

(12) Dettlaff-Weglikowska, U.; Hönle, W.; Molassioti-Dohms, A.; Finkbeiner, S.; Weber, J. Structure and Optical Properties of the Planar Silicon Compounds Polysilane and Wöhler Siloxene. *Phys. Rev. B* **1997**, *56*, 13132−13140.

(13) Bianco, E.; Butler, S.; Jiang, S.; Restrepo, O. D.; Windl, W.; Goldberger, J. E. Stability and Exfoliation of Germanane: A Germanium Graphane Analogue. *ACS Nano* **2013**, *7*, 4414−4421.

(14) Jiang, S.; Butler, S.; Bianco, E.; Restrepo, O. D.; Windl, W.; Goldberger, J. E. Improving the Stability and Optical Properties of Germanane via One-Step Covalent Methyl-Termination. *Nat. Commun.* **2014**, *5*, No. 3389.

(15) Xu, Y.; Yan, B.; Zhang, H.-J.; Wang, J.; Xu, G.; Tang, P.; Duan, W.; Zhang, S.-C. Large-Gap Quantum Spin Hall Insulators in Tin Films. *Phys. Rev. Lett.* **2013**, *111*, No. 136804.

(16) Knapp, D. Chemistry and Electronics of the Ge(111) Surface, Doctor of Philosophy thesis, California Institute of Technology, 2011.

DOI: 10.1021/ar500296e
Acc. Chem. Res. 2015, 48, 144−151

(17) Bansal, A.; Li, X.; Lauermann, I.; Lewis, N. S.; Yi, S. I.; Weinberg, W. Alkylation of Si Surfaces Using a Two-step Halogenation/Grignard Route. *J. Am. Chem. Soc.* **1996**, *118*, 7225−7226.
(18) Han, S. M.; Ashurst, W. R.; Carraro, C.; Maboudian, R. Formation of Alkanethiol Monolayer on Ge (111). *J. Am. Chem. Soc.* **2001**, *123*, 2422−2425.
(19) Linford, M. R.; Fenter, P.; Eisenberger, P. M.; Chidsey, C. E. Alkyl Monolayers on Silicon Prepared from 1-Alkenes and Hydrogen-terminated Silicon. *J. Am. Chem. Soc.* **1995**, *117*, 3145−3155.
(20) Buriak, J. M. Organometallic Chemistry on Silicon and Germanium Surfaces. *Chem. Rev.* **2002**, *102*, 1271−1308.
(21) Carberry, E.; Dombek, B. D. Cyclic Heteroatom Permethylpolysilanes I. Dodecamethylgermacyclohexasilane and Dodecamethyl-1,4-Digermacyclohexasilane. *J. Organomet. Chem.* **1970**, *22*, c43−c47.
(22) Carberry, E.; Dombek, B. D.; Cohen, S. C. The Preparation and Spectroscopic Properties of the Permethylcyclopolygermanes. *J. Organomet. Chem.* **1972**, *36*, 61−70.
(23) Adams, S.; Dräger, M. Polystannanes Ph_3Sn-$(tBu_2Sn)_n$-Ph_3 (n=1−4): A Route to Molecular Metals? *Angew. Chem., Int. Ed.* **1987**, *26*, 1255−1256.
(24) Wöhler, F. Ueber Verbindungen des Siliciums mit Sauerstoff und Wasserstoff. *Justus Liebigs Ann. Chem.* **1863**, *127*, 257−274.
(25) Kautsky, H. Über einige ungesättigte Siliciumverbindungen. *Z. Anorg. Allg. Chem.* **1921**, *117*, 209−242.
(26) Kautsky, H.; Herzberg, G. Über das Siloxen und seine Derivate. *Z. Anorg. Allg. Chem.* **1924**, *139*, 135−160.
(27) Weiss, A.; Beil, G.; Meyer, H. The Topochemical Reaction of $CaSi_2$ to a Two-Dimensional Subsiliceous Acid $Si_6H_3(OH)_3$ (=Kautskys' Siloxene). *Z. Naturforsch., B* **1980**, *35b*, 25−30.
(28) Brandt, M.; Puchert, T.; Stutzmann, M. Electronic Transport in Crystalline Siloxene. *Solid State Commun.* **1997**, *102*, 365−368.
(29) Dahn, J. R.; Way, B. M.; Fuller, E.; Tse, J. S. Structure of Siloxene and Layered Polysilane (Si_6H_6). *Phys. Rev. B* **1993**, *48*, 17872−17877.
(30) Okamoto, H.; Kumai, Y.; Sugiyama, Y.; Mitsuoka, T.; Nakanishi, K.; Ohta, T.; Nozaki, H.; Yamaguchi, S.; Shirai, S.; Nakano, H. Silicon Nanosheets and Their Self-assembled Regular Stacking Structure. *J. Am. Chem. Soc.* **2010**, *132*, 2710−2718.
(31) Nakano, H.; Nakano, M.; Nakanishi, K.; Tanaka, D.; Sugiyama, Y.; Ikuno, T.; Okamoto, H.; Ohta, T. Preparation of Alkyl-modified Silicon Nanosheets by Hydrosilylation of Layered Polysilane (Si_6H_6). *J. Am. Chem. Soc.* **2012**, *134*, 5452−5455.
(32) Sugiyama, Y.; Okamoto, H.; Mitsuoka, T.; Morikawa, T.; Nakanishi, K.; Ohta, T.; Nakano, H. Synthesis and Optical Properties of Monolayer Organosilicon Nanosheets. *J. Am. Chem. Soc.* **2010**, *132*, 5946−5947.
(33) Vogg, G.; Brandt, M. S.; Stutzmann, M. Polygermyne—A Prototype System for Layered Germanium Polymers. *Adv. Mater.* **2000**, *12*, 1278−1281.
(34) Jiang, S.; Bianco, E.; Goldberger, J. E. The Structure and Amorphization of Germanane. *J. Mater. Chem. C* **2014**, *2*, 3185−3188.
(35) Arguilla, M. Q.; Jiang, S.; Chitara, B.; Goldberger, J. E. Synthesis and Stability of Two-dimensional Ge/Sn Graphane Alloys. *Chem. Mater.* **2014**, DOI: 10.1021/cm502755q.
(36) Frindt, R.; Yoffe, A. Physical Properties of Layer Structures: Optical Properties and Photoconductivity of Thin Crystals of Molybdenum Disulphide. *Proc. R. Soc. A* **1963**, *273*, 69−83.
(37) Novoselov, K.; Jiang, D.; Schedin, F.; Booth, T.; Khotkevich, V.; Morozov, S.; Geim, A. Two-dimensional Atomic Crystals. *Proc. Natl. Acad. Sci. U. S. A.* **2005**, *102*, 10451−10453.
(38) Pinchuk, I. V.; Odenthal, P. M.; Ahmed, A. S.; Amamou, W.; Goldberger, J. E.; Kawakami, R. K. Epitaxial Co-deposition Growth of $CaGe_2$ Films by Molecular Beam Epitaxy for Large Area Germanane. *J. Mater. Res.* **2014**, *29*, 410−416.
(39) He, J.; Lu, Z.-H.; Mitchell, S. A.; Wayner, D. D. Self-assembly of Alkyl Monolayers on Ge (111). *J. Am. Chem. Soc.* **1998**, *120*, 2660−2661.
(40) Nemanick, E. J.; Hurley, P. T.; Brunschwig, B. S.; Lewis, N. S. Chemical and Electrical Passivation of Silicon (111) Surfaces through Functionalization with Sterically Hindered Alkyl Groups. *J. Phys. Chem. B* **2006**, *110*, 14800−14808.
(41) Deak, P.; Rosenbauer, M.; Stutzmann, M.; Weber, J.; Brandt, M. S. Siloxene: Chemical Quantum Confinement Due to Oxygen in a Silicon Matrix. *Phys. Rev. Lett.* **1992**, *69*, 2531−2534.
(42) Restrepo, O. D.; Mishra, R.; Goldberger, J. E.; Windl, W. Tunable Gaps and Enhanced Mobilities in Strain-Engineered Silicane. *J. Appl. Phys.* **2014**, *115*, No. 033711.
(43) Lew Yan Voon, L. C.; Sandberg, E.; Aga, R. S.; Farajian, A. A. Hydrogen Compounds of Group-IV Nanosheets. *Appl. Phys. Lett.* **2010**, *97*, No. 163114.
(44) Nakano, H.; Mitsuoka, T.; Harada, M.; Horibuchi, K.; Nozaki, H.; Takahashi, N.; Nonaka, T.; Seno, Y.; Nakamura, H. Soft Synthesis of Single-crystal Silicon Monolayer Sheets. *Angew. Chem., Int. Ed.* **2006**, *45*, 6303−6306.
(45) Paier, J.; Marsman, M.; Hummer, K.; Kresse, G.; Gerber, I. C.; Angyan, J. G. Screened Hybrid Density Functionals Applied to Solids. *J. Chem. Phys.* **2006**, *124*, No. 154709.
(46) Heyd, J.; Scuseria, G. E.; Ernzerhof, M. Hybrid Functionals Based on a Screened Coulomb Potential. [Erratum to Document Cited in CA139:042043]. *J. Chem. Phys.* **2006**, *124*, No. 219906.
(47) Macfarlane, G. G.; Roberts, V. Infrared Absorption of Germanium Near the Lattice Edge. *Phys. Rev.* **1955**, *97*, 1714−1716.
(48) Clark, C. D.; Dean, P. J.; Harris, P. V. Intrinsic Edge Absorption in Diamond. *Proc. R. Soc. A* **1964**, *277*, 312−329.
(49) Lebegue, S.; Klintenberg, M.; Eriksson, O.; Katsnelson, M. I. Accurate Electronic Band Gap of Pure and Functionalized Graphane from GW Calculations. *Phys. Rev. B* **2009**, *79*, No. 245117.
(50) Bludau, W.; Onton, A.; Heinke, W. Temperature Dependence of the Band Gap of Silicon. *J. Appl. Phys.* **1974**, *45*, 1846−1848.
(51) Hoechst, H.; Hernandez-Calderon, I. Angular Resolved Photoemission of Indium Antimonide(001) and Heteroepitaxial Films of α-Sn(001). *Surf. Sci.* **1983**, *126*, 25−31.
(52) Rivillon, S.; Chabal, Y. J.; Amy, F.; Kahn, A. Hydrogen Passivation of Germanium (100) Surface Using Wet Chemical Preparation. *Appl. Phys. Lett.* **2005**, *87*, No. 253101.

DOI: 10.1021/ar500296e
Acc. Chem. Res. 2015, 48, 144−151